

# Thermal Behavior and Molecular Orientation of Poly(ethylene 2,6-naphthalate) in Thin Films

Ying Zhang,<sup>†</sup> Shota Mukoyama,<sup>†</sup> Yun Hu,<sup>‡</sup> Chao Yan,<sup>†</sup> Yukihiro Ozaki,<sup>‡</sup> and Isao Takahashi<sup>\*,†</sup>

Department of Physics, School of Science and Technology, Kwansei Gakuin University, Sanda, Hyogo 669-1337, Japan, and Department of Chemistry, School of Science and Technology, Kwansei Gakuin University, Sanda, Hyogo 669-1337, Japan

Received January 4, 2007; Revised Manuscript Received March 16, 2007

**ABSTRACT:** Studies on structural orientation of polymers near the surface and interface or in confined geometry mostly dealt with the resulting anisotropic arrangements of the involving polymer molecule. The molecular dynamics during the orientation process of a target polymer was, however, not concerned so far. In the present study, molecular orientation of poly(ethylene 2, 6-naphthalate) (PEN) thin films during isothermal and nonisothermal crystallization was investigated by the combination of in situ reflection–absorption infrared spectroscopy (RAIR) and grazing incidence X-ray diffraction (GIXD) techniques. The results disclose that the naphthalene ring and C=O in PEN molecule is prone to alignment parallel to the film surface during the formation of  $\alpha$ -form crystalline. In situ RAIR measurements further suggest that the kinetics of molecular orientation exhibits clearly different from that of crystallization. In situ GIXD experiments done by synchrotron radiation also reveal the structural developing process during the orientation, in which the naphthalene ring rotates to be more parallel to the surface than the lattice plane containing *b* and *c* axes. Furthermore, the possible mechanisms for the observed orientation in PEN thin films are also discussed.

## 1. Introduction

In recent years as thin (thickness <500 nm) and ultrathin (thickness <100 nm) polymer films become more desirable in technological applications such as microelectronics fabrication, liquid crystal displays, photoresists for photolithography, and adhesive or passivation layers, understanding the roles of confinement and interface in altering the physical behavior of polymers is of great importance. The confinement of polymers in thin films, block copolymers, or nanocomposites is known to significantly alter numerous physical properties, such as glass transition temperature,<sup>1–3</sup> crystallization behavior,<sup>4,5</sup> phase behavior and morphology,<sup>6–8</sup> and electrical properties,<sup>9</sup> etc. In particular, experimental evidence accumulated so far<sup>5,10–12</sup> shows that the presence of a surface and the confined geometry are also very important factors determining the molecular orientation of ultrathin or thin polymer films. Preferential alignment of macromolecules in thin polymer films was first reported by Prest and Luca,<sup>10</sup> who pointed out that the polymer chains were oriented in the plane of the coating in solvent-cast films. Studies conducted by Frank et al.<sup>5,11</sup> also revealed that while the backbones of poly(di-*n*-hexylsilane) deposited on quartz substrate are aligned preferentially in the plane of the film, the mean orientation of poly(ethylene oxides) (PEO) molecules on an oxidized silicon substrate is in the surface-normal direction. Furthermore, they found that the PEO lamellar crystal shows an interesting film-thickness-dependent morphology and orientation. A higher degree of orientation of the polymer chains in proximity to the substrate was also reported by Cohen and Reich<sup>12</sup> for dip-coated films.

Several experimental techniques have been developed to offer the possibility for detecting the molecular structure and orientation confined in thin polymer films. Among them, Fourier transform infrared (FTIR) spectroscopy is a powerful technique and has great advantage: it can probe directly to such subtle details as intermolecular interactions, localized molecular conformations and orientations. As one of various kinds of infrared techniques, reflection–absorption infrared (RAIR) spectroscopy fits sufficiently to the characterization of ultrathin films with the thickness of nanometer scale. The characteristic<sup>13</sup> of RAIR is that the resultant electric field vector is perpendicular to the metal-based surface. Therefore, if molecules are adsorbed onto the substrate with a preferred orientation, vibration modes having transition moments perpendicular to the surface will appear with greater intensity than modes having transition moments parallel to the surface. Thus, RAIR is especially useful for determining the orientation of adsorbed molecular species. A technique of grazing incidence X-ray diffraction (GIXD) also enables us to gain direct access to information on surface and bulk ordering.<sup>14–18</sup> One of the principal advantages of the technique is that the structure both in the plane and out of the plane of a sample surface can be probed by employing one of two different scattering geometries. That is, by collecting Bragg reflections from the crystals under the in-plane and out-of-plane scanning conditions, the corresponding information on crystal-line structure along normal and parallel to the sample surface can be obtained. The combination of RAIR and GIXD will undoubtedly provide unmatched advantage on exploring the orientational structure in confined geometry even though such kind of work is still very rare.

Despite of much effort deployed to characterize the molecular orientation of polymer by means of variable techniques, the details of the development and origin of orientation process still remain unrevealed. In the present study, RAIR and GIXD are employed to detect the molecular orientation in thin films of

\* To whom all correspondence should be addressed. E-mail: z96019@ksc.kwansei.ac.jp.

<sup>†</sup> Department of Physics, School of Science and Technology, Kwansei Gakuin University.

<sup>‡</sup> Department of Chemistry, School of Science and Technology, Kwansei Gakuin University.

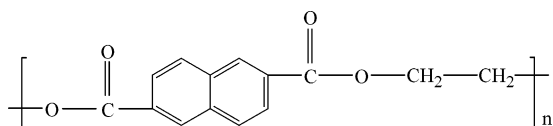


**Figure 1.** Chemical structure of poly(ethylene 2,6-naphthalate) (PEN).

poly(ethylene 2,6-naphthalate) (PEN), which is a high performance thermoplastic polyester with a rigid naphthalene ring and a flexible aliphatic diol unit (see Figure 1). Specifically, the real time developing process of the molecular orientation in PEN thin films is investigated by using in situ RAIR and GIXD methods. The purpose of this paper is to present some detailed experimental results regarding the structural changes during orientation in thin films of PEN in the course of isothermal and nonisothermal crystallization.

## 2. Experimental Section

**2.1. Sample Preparation.** PEN sample with an intrinsic viscosity of 0.50 dL/g was kindly supplied by Prof. Deyan Shen of Institute of Chemistry, Chinese Academy of Sciences. The PEN pellets were dissolved in chloroform-trifluoroacetic acid (volume ratio 1:1). Substrates of silicon (100) wafers and gold-coated glass wafers were used to prepare thin PEN films for GIXD and RAIR measurements, respectively (see ref 19 for detailed procedures of cleaning the substrates). Thin films with different thickness were prepared by spin-coating the PEN solutions of various concentrations at several speeds for about 60 s onto the gold-coated glass wafers and silicon (100) wafers. The films were kept under vacuum at 40 °C for 24 h to remove the residual solvent.

The thicknesses of thin PEN films with low roughness on the silicon wafers were determined by a fit of the X-ray reflectivity data with a self-made software in which a recursive method based on the dynamical scattering theory was employed.<sup>20</sup> Thickness measurements of thin PEN films with high roughness were performed with Nanopics 1000 atomic force microscope (AFM) (Seiko Instruments Inc.) in tapping mode. The film thickness was determined by AFM height profile after partially removing the thin films from the substrates. They were defined as the distance between the substrates surface and the average of all height values taken in a line scan across the sample surface.<sup>21</sup> To minimize the experimental errors, several height profiles taken from different locations of one sample were averaged.

Thick films of PEN for attenuated total reflection FT-IR (ATR) measurements were produced by thermally pressing PEN pellets between two pieces of aluminum foil at about 290 °C and then quenched to liquid nitrogen. The films covered by aluminum foils were immersed into NaOH solution to remove the aluminum foils. Before the ATR measurements, the films were washed by deionized water and then dried at 40 °C for 24 h. Thicknesses of the obtained film were about 50  $\mu\text{m}$  (estimated by using area after pressing, weight, and density of PEN used). PEN thick films for GIXD measurements were prepared by casting concentrated solution of PEN on silicon (100) wafers, and then evaporated in a vacuum oven at 40 °C for 24 h. Thicknesses of the thick films were about 30  $\mu\text{m}$  (estimated by using the casting weight of solution, deposit area and the density of PEN used).

**2.2. RAIR and ATR Measurements.** RAIR and ATR spectra in the region of 4000–400  $\text{cm}^{-1}$  were collected with a Thermo Nicolet Magna 470 spectrometer equipped with a mercury cadmium telluride (MCT) detector. The measurements were carried out at a resolution of 4  $\text{cm}^{-1}$  by averaging 32 scans. For RAIR measurements, the incidence angle was fixed at 84° for the best signal recording. The polarization of the incoming beam was parallel to the plane of incidence (p-polarized, by using a reumatically rotatable wire-grid polarizer of ST Japan). All RAIR spectra were obtained by subtracting the spectrum of Au substrate without sample from the spectrum of a PEN-film-covered Au substrate. A homemade heating stage with accuracy of  $\pm 0.3$  °C was used to

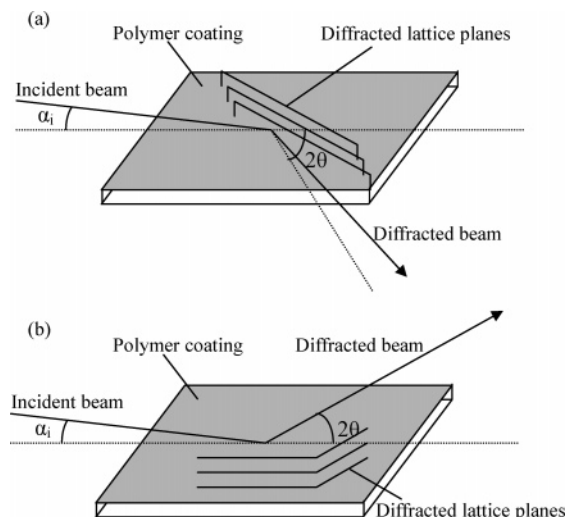


**Figure 2.** Schematic representations of (a) in-plane and (b) out-of-plane GIXD measurements.

obtain in situ FTIR spectra. During the RAIR measurements of isothermal crystallization, the time interval was 2 min for each scan.

ATR measurements were carried out by using a multiple reflection ATR accessory (Spectra Tech, USA) with a 45° ZnSe IRE (10  $\times$  75.5  $\times$  3 mm). A wire-grid polarizer (ST Japan) was also employed to record the infrared spectra with p-polarized direction. The effective depth of penetration ( $de(P_{||})$ ) is determined by eq 1,<sup>22</sup> where  $n_{21} = n_{\text{polymer}}/n_{\text{crystal}}$ ,  $\lambda_1 = \lambda/n_{\text{crystal}}$ , and  $n$ ,  $\lambda$ , and  $\theta$  are the refractive index, wavelength, and the incident angle, respectively

$$\frac{de(P_{||})}{\lambda_1} = \frac{n_{21} \cos \theta (2 \sin^2 \theta - n_{21}^2)}{\pi (1 - n_{21}^2) [(1 + n_{21}^2) \sin^2 \theta - n_{21}^2] (\sin^2 \theta - n_{21}^2)^{1/2}} \quad (1)$$

**2.3. X-ray Diffraction.** The crystalline structure of PEN thin films was investigated by GIXD measurements. The measurements were carried out using a diffractometer (TTR-450, Rigaku Co. Ltd.) with a rotating Cu anode X-ray source ( $\lambda = 1.5406 \text{ \AA}$ ). The size of the incident beam was defined by a collimator with diameter of 1 mm. A soller slit was placed before a scintillation detector to collimate the scattered beam. The fixing time for data collection was 60 s per step, and the angular interval was 0.05°. The samples were mounted on a four-circle goniometer with the film plane nearly horizontal. The GIXD measurements were performed with in-plane and out-of-plane configuration to detect the crystalline structure of perpendicular and parallel to the substrate surface, respectively. The schematic pictures of in-plane and out-of-plane GIXD measurements are shown in Figure 2. In order to obtain real time information about the crystalline structure of polymer thin film during the heating and cooling process, synchrotron radiation and multiaxis diffractometer at the BL13XU beamline of SPring-8 was employed. The wavelength of monochromatized incident X-ray was 0.7  $\text{\AA}$ . The beam sizes at incident slits were 0.2 and 0.5 mm in the vertical and horizontal directions respectively. The fixing time for data collection was 1 s per step, and the angular interval was 0.04°. For studying the thermal behavior of PEN thin films via in situ GIXD, a homemade heater with accuracy of  $\pm 0.3$  °C was used.

## 3. Results and Discussion

To investigate the preferred orientation of PEN molecule in the thin film during crystallization, RAIR spectra of a 150 nm PEN film before and after isothermally crystallized at 210 °C for 2 h from glassy state were compared, as displayed in Figure 3a. It is well-known that PEN can crystallize into at least two different crystal modifications, i.e., the  $\alpha$  and  $\beta$  forms.<sup>23,24</sup> The  $\alpha$  crystal form can be obtained by annealing amorphous PEN

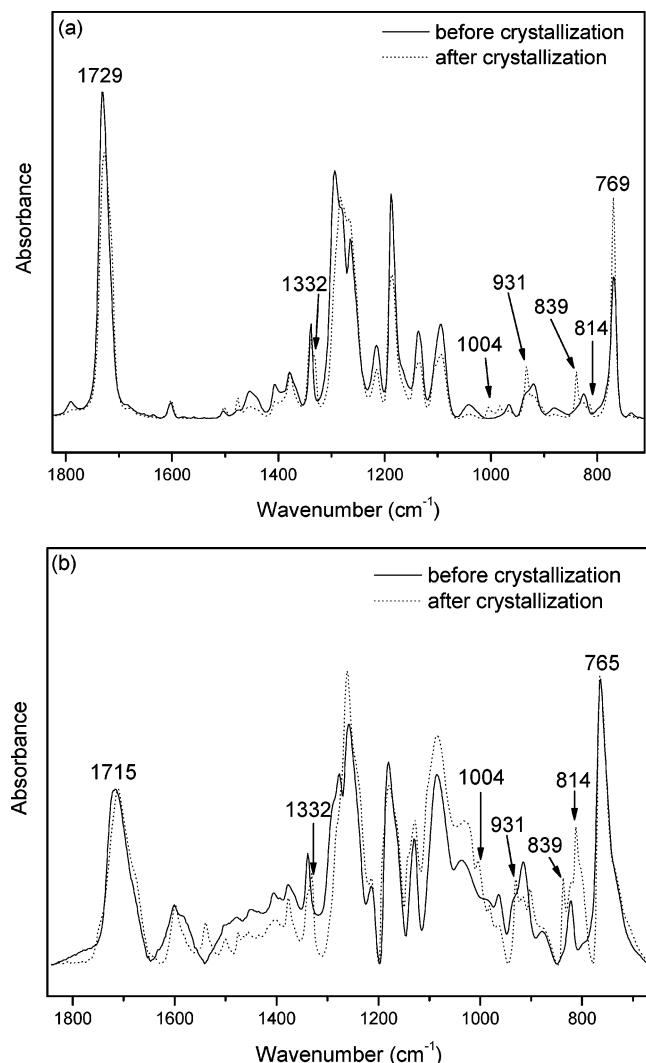


**Figure 3.** Infrared spectra of PEN before and after isothermal cold crystallization at 210 °C for 2 h by (a) RAIR for a 150 nm thin film and (b) ATR for a 50  $\mu\text{m}$  pressed thick film (the spectra were normalized by film thickness to be comparable).

**Table 1.** Assignment and Polarization of IR Band of PEN

wavenumber ( $\text{cm}^{-1}$ ) <sup>a</sup>	band assignment <sup>b,c</sup>	polarization <sup>c,d</sup>
1729 (1715)	$\nu(\text{C}=\text{O})$	$\perp, \pi$
1332	$\omega(\text{CH}_2)$ trans	//
1092	$\nu_s(\text{C}-\text{O})$ gauche	//
1004	crystalline	
931	$\delta(\text{ring CH out-of-plane})$	$\perp$
839	crystalline	$\perp$
814	crystalline	//
769 (765)	$\delta(\text{ring CH out-of-plane})$	$\perp, \sigma$

<sup>a</sup> The wavenumbers in bracket represent the peak positions in transmission IR spectra. <sup>b</sup>  $\nu$  = stretching,  $\omega$  = wagging,  $\nu_s$  = symmetry stretching, and  $\delta$  = deformation. <sup>c</sup> Reference 25. <sup>d</sup>  $\perp$  and // denote perpendicular and parallel polarization, respectively, with respect to the main-chain axis of PEN molecules.  $\pi$  and  $\sigma$  denote parallel and perpendicular to the plane of the naphthalene ring respectively.

in the solid state, while the crystal form  $\beta$  can be obtained directly from the melt. It can be concluded from the appearance of characteristic bands at 814, 839, 931, 1004, and 1332  $\text{cm}^{-1}$  (see Table 1 for assignment of the IR band of PEN) for the spectrum of crystallized PEN thin film that the  $\alpha$ -form crystalline structure is formed.<sup>25</sup> Figure 3a further indicates that the bands of C=O stretching at 1729  $\text{cm}^{-1}$  and ring CH out-of-plane deformation at 769  $\text{cm}^{-1}$  display difference in the relative intensities. After crystallization, the intensity of 1729  $\text{cm}^{-1}$  band

decreases while that of 769  $\text{cm}^{-1}$  band increases. As summarized in Table 1, both of these two bands show perpendicular polarization. However, the transition moment of 1729  $\text{cm}^{-1}$  band is parallel to the plane of naphthalene ring while it is perpendicular to the plane for the transition moment of 769  $\text{cm}^{-1}$  band.<sup>25</sup> Considering the facts that the main-chain of PEN in thin film state shows alignment parallel to the substrate,<sup>26</sup> and all the atoms of the polymer chain including O=C-O and naphthalene ring (except the hydrogens of  $\text{CH}_2$ ) are coplanar after crystallization in PEN,<sup>25</sup> it is thus concluded from the relative change in intensity of the above two bands that both the naphthalene ring and carbonyl group in PEN molecular chain tend to be aligned preferentially parallel to the substrate during crystallization.

Polarized ATR measurements were also carried out to detect the possible orientation that exists in bulk PEN. Here we used the parallel polarized light (p-polarized), which is the same as that of the RAIR measurements. The effective depth of penetration ( $de(P_{\parallel})$ ) can be determined by eq 1. For the present study, the refractive index of PEN is about 1.62, and the refractive index of ZnSe IRE internal reflection crystal ( $n_{\text{crystal}}$ ) is 2.403.<sup>27</sup> Therefore, the effective depths for the  $P_{\parallel}$  ( $de(P_{\parallel})$ ) lights were calculated to be 4.1 and 1.8  $\mu\text{m}$ , respectively at 765 and 1715  $\text{cm}^{-1}$ , which are thick enough to reflect the structural information throughout the bulk PEN. Figure 3b gives the ATR spectra of a hot-pressed PEN thick film before and after isothermally crystallized at 210 °C for 2 h from glassy state. It is known that the ATR spectra differ from transmission or reflectance spectra on the fact that the absorbance of ATR bands increase with the wavelength.<sup>22</sup> The phenomenon is indeed observed from the peak absorbance in the 700–1800  $\text{cm}^{-1}$  region in Figure 3b. Similar to the spectrum of PEN thin film in Figure 3a, the characteristic bands of  $\alpha$ -form crystalline at 814, 839, 931, 1004, and 1332  $\text{cm}^{-1}$  can also be observed from the spectrum of crystallized PEN thick film in Figure 3b. However, when the spectra of PEN before and after crystallized were further compared, very little difference in absorbance can be found at 1715  $\text{cm}^{-1}$  for C=O stretching and at 765  $\text{cm}^{-1}$  for ring CH out-of-plane deformation. The result indicates that the preferred orientation of naphthalene ring and carbonyl group that exists in thin film can hardly occur in bulk PEN film.

Because the observed anisotropic structure in PEN thin film occurs in crystalline, questions may be raised on how does the orientation develop accompanying by the crystallization process, and whether this kind of ordering (or orientation) is a chain alignment precursor effect in thin film that precedes normal crystallization. To make these questions clear, the in situ RAIR experiments were performed during the isothermal crystallization from glassy of PEN thin films. The measurements were conducted at 145 °C from glassy for about 118 min. Figure 4 shows time-dependent RAIR spectra of a PEN thin film with thickness of about 150 nm during isothermal crystallization. For clarity, we only give the wavenumber regions in which several typical bands, concerning the orientation and  $\alpha$ -form crystallization (or conformation) (that is, 1729, 1092, 839, 814, and 769  $\text{cm}^{-1}$  bands) are displayed. By adopting the orientation-sensitive and crystallization (or conformation)-sensitive bands, it is possible for us to follow the detailed developments of structural changes during orientation and crystallization respectively. As mentioned above, due to the strong polarization of the C=O stretching band at 1729  $\text{cm}^{-1}$  and ring CH out-of-plane deformation band at 769  $\text{cm}^{-1}$ , the intensity change of these two bands in RAIR during crystallization should be caused mainly by the molecular orientation of PEN. During the



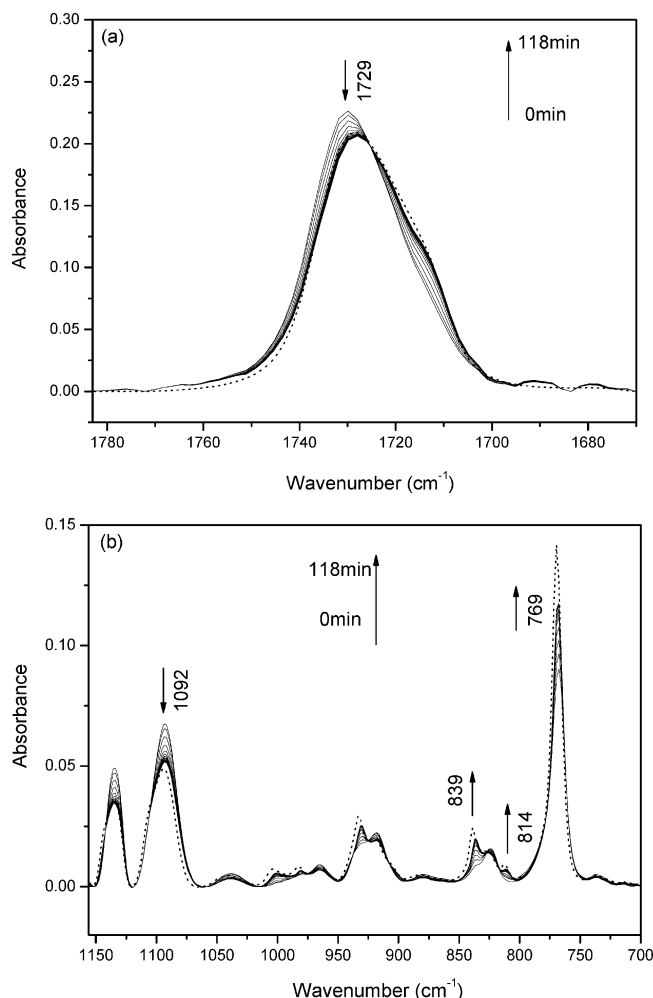


**Figure 4.** Temporal changes of the RAIR spectrum in the regions of (a) 1780–1670 and (b) 1150–700  $\text{cm}^{-1}$  during isothermal cold crystallization of PEN thin film with thickness of about 150 nm at 145  $^{\circ}\text{C}$ . The spectra of PEN thin films after cooling to room temperature are given as dot lines.

isothermal crystallization at 145  $^{\circ}\text{C}$ , the intensity of the 1729  $\text{cm}^{-1}$  band decreases while that of the 769  $\text{cm}^{-1}$  band increases, as is shown in Figure 4, parts a and b. The band at 1092  $\text{cm}^{-1}$  can be assigned as symmetric C–O stretching vibration of the gauche conformer.<sup>25</sup> In amorphous regions the  $-\text{O}-\text{CH}_2-\text{CH}_2-\text{O}-$  moiety in PEN usually adopts gauche conformation with some small contribution of trans conformation, while in crystalline regions it is mainly in a trans conformation. Therefore, the 1092  $\text{cm}^{-1}$  band decreases in absorbance significantly during crystallization.<sup>25,28</sup> As for the 839 and 814  $\text{cm}^{-1}$  bands, Ouchi et al.<sup>25</sup> attributed these two bands to the crystalline splitting due to intermolecular interactions. From the assignment it can be expected that the 1092  $\text{cm}^{-1}$  band decrease in absorbance while the 839 and 814  $\text{cm}^{-1}$  bands increase during the crystallization. These are really observed in Figure 4.

To obtain more quantitative description about the orientation and crystallization process, plots that give the time dependence of the peak intensities for the 1729, 1092, 839, and 769  $\text{cm}^{-1}$  bands in RAIR spectra of the PEN thin film isothermally crystallized at 145  $^{\circ}\text{C}$  are made and shown in Figure 5. It can be seen from Figure 5 that the kinetics during isothermal crystallization are clearly different between the orientation-sensitive bands (1729 and 769  $\text{cm}^{-1}$  bands) and the crystallization (or conformation)-sensitive bands (1092 and 839  $\text{cm}^{-1}$  bands). The changes in absorbance for the 1729 and 769  $\text{cm}^{-1}$  bands exhibit faster speed to achieve a steady state than those

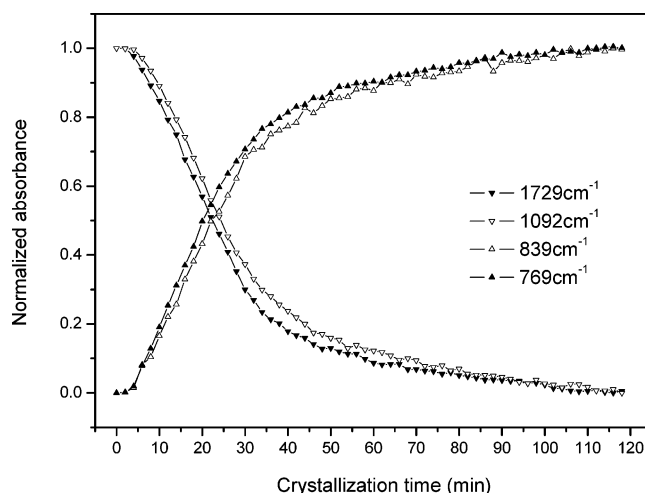


**Figure 5.** Normalized intensities of the bands at 1729, 1092, 839, and 769  $\text{cm}^{-1}$  as a function of time during isothermal cold crystallization at 145  $^{\circ}\text{C}$ .

of the 1092 and 839  $\text{cm}^{-1}$  bands. Among these bands, the intensity change at 1092  $\text{cm}^{-1}$  should also be correlated with crystallization process, even though this kind of band is primarily sensitive to the conformation.<sup>29</sup> Because during the course of crystalline formation (from the appearance of the typical bands for crystalline at 839 and 814  $\text{cm}^{-1}$  in Figure 4) at 145  $^{\circ}\text{C}$  for PEN thin film, the change in conformation should be mainly caused by crystallization. Such kind of conformation-sensitive band serving as “crystallization-sensitive” band can also be found in other studies.<sup>28,30</sup> The experimental result shown in Figure 5 may reflect the substantial difference between the orientation and the crystallization in the course they develop: the former can only reflect the specific arrangement of molecular structure, while more complex factors such as nucleation and growth of crystals may also be involved in the latter. In addition, from Figure 5, especially from the plots of 1729 and 1092  $\text{cm}^{-1}$  bands, it can be observed that the changes of bands corresponding to molecular orientation and crystallization display different at the starting points: the orientation takes place prior to the crystallization. This can also be observed in a recent study of PCL/PE system.<sup>31</sup>

The spectra of PEN thin films cooling to room temperature after crystallization were also recorded. They are given as dot lines in Figure 4, parts a and b. It is noted that the bands at 769, 839, and 1092  $\text{cm}^{-1}$  show further changes in absorbance compared with those at high temperatures: the intensities of the 769 and 839  $\text{cm}^{-1}$  bands increase, while the intensity of the 1092  $\text{cm}^{-1}$  band decreases. This kind of intensity changes during cooling process should be associated with the further perfection of crystalline or secondary crystallization.<sup>32</sup> Our results in Figure 4 indicate that a remarkable increase takes place for both the crystallinity of PEN thin film and the orientation of naphthalene ring when cooling from 145  $^{\circ}\text{C}$  to room temperature. The intensity of 1729  $\text{cm}^{-1}$  band, on the other hand, shows relatively little difference when suffering the same cooling treatment. It was reported<sup>33,34</sup> that the C=O stretching vibration of PEN usually shifts to a lower wavenumber during crystallization. Kimura et al.<sup>33</sup> explained this kind of downward band shift by the difference in coplanarity of the C=O group with respect to the naphthalene ring. They suggested that conjugation has a strong electron-withdrawing effect on the C=O group, leading to a band shift to the lower wavenumber in the vibration. The band shift for the C=O group was also found obviously during isothermal crystallization of PEN at 145  $^{\circ}\text{C}$  in the present

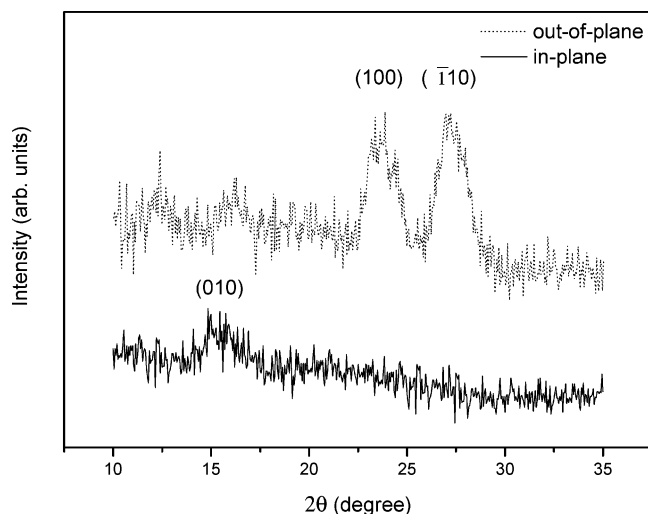


**Figure 6.** Out-of-plane and in-plane GIXD profiles of a 150 nm PEN thin film after isothermal cold crystallization at 210 °C for 2 h (incident angle  $\alpha = 0.175^\circ$ ).

study, as shown in Figure 4a. However, for subsequent cooling process, only a slight downward band shift can be observed for this band. Associated with the fact that both the intensity and peak position take significant changes for the ring vibration at  $769\text{ cm}^{-1}$ , the present experimental results probably indicate that the naphthalene ring rather than the C=O group takes more orientation to contribute to the coplanarity during the cooling process.

The GIXD results can also provide us detailed information about the structural changes during orientation of PEN thin films. Figure 6 shows the out-of-plane and in-plane GIXD profiles of a 150 nm PEN ultrathin film after isothermal crystallization from glassy at 210 °C for 2 h. Since the incident angle was kept at  $0.175^\circ$ , which is above the critical angle of  $0.15^\circ$  (in the case of  $\lambda = 1.5406\text{ \AA}$ ), the resulting profiles fully contains structural information deep in the films. As mentioned above, PEN has been reported to have at least two modifications, i.e., the  $\alpha$  and  $\beta$  forms. The unit cell of the  $\alpha$  form was determined by Mencik<sup>23</sup> as triclinic with  $a = 0.651\text{ nm}$ ,  $b = 0.575\text{ nm}$ ,  $c = 1.32\text{ nm}$ ,  $\alpha = 81.33^\circ$ ,  $\beta = 144^\circ$ , and  $\gamma = 100^\circ$ . A triclinic unit cell was also proposed by Zachmann<sup>24</sup> for the  $\beta$  crystal form with  $a = 0.926\text{ nm}$ ,  $b = 1.559\text{ nm}$ ,  $c = 1.273\text{ nm}$ ,  $\alpha = 121.6^\circ$ ,  $\beta = 95.57^\circ$ , and  $\gamma = 122.52^\circ$ . The present GIXD result shows the crystalline reflections of (100), (110), and (010) plane ( $2\theta$  are 23.3, 27.0, and  $15.6^\circ$ , respectively), which are major reflections of the  $\alpha$ -form crystal. This indicates the formation of  $\alpha$ -form crystal and agrees with the conclusion obtained from the RAIR measurements. Furthermore, out-of-plane and in-plane profiles show quite different relative intensity of each diffraction peak. While the out-of-plane scattering is dominated by the (100) and (110) peaks, the in-plane scattering is dominated by a unique Bragg peak: (010) peak. These results clearly indicate that the crystals formed during the present crystallization process are highly anisotropic, and hence preferential orientation occurs throughout the PEN ultrathin film. Since the (110) lattice plane is approximately parallel to the naphthalene ring in PEN molecule (making an angle of about  $4.7^\circ$  with the naphthalene ring),<sup>35</sup> it can be inferred that the naphthalene ring plane is almost parallel to the film surface in the crystalline region from the presence of (110) Bragg peak only in the out-of-plane scan. This is consistent with the result derived from the RAIR spectra. The  $c$ -axis (main chain of PEN molecule) can also be proved to align along the direction parallel to the sample surface in terms of the comparison of IR

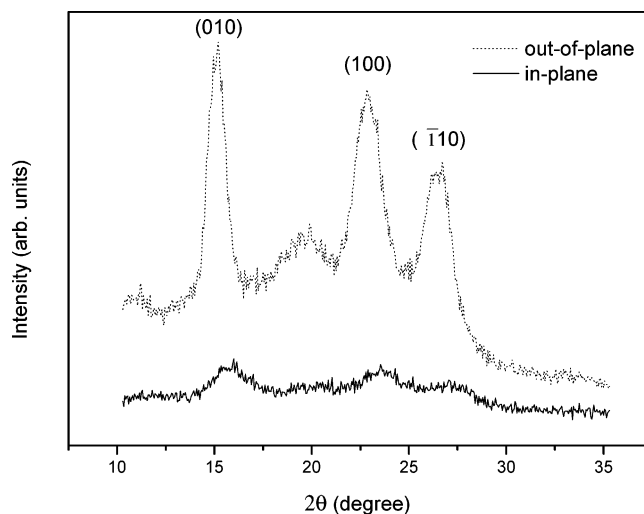


**Figure 7.** Out-of-plane and in-plane GIXD profiles of a  $30\text{ }\mu\text{m}$  solution-cast PEN film after isothermal crystallization at 210 °C for 2 h (incident angle  $\alpha = 1^\circ$ ).

transmission and RAIR spectra.<sup>26</sup> Moreover, in the case of out-of-plane geometry, the intensity of (100) reflection displays very strong in peak intensity, while this peak cannot be observed for the in-plane geometry. This result reveals that the  $b$ -axis in the PEN ultrathin film is also preferentially more parallel to the film surface. To make clear whether this kind of anisotropic arrangement in PEN crystalline also exists in bulk PEN, the out-of-plane and in-plane GIXD profiles of a crystallized solution-cast PEN film with the thickness of about  $30\text{ }\mu\text{m}$  was recorded and shown in Figure 7. The figure discloses that in both out-of-plane and in-plane profiles the (010) Bragg diffraction becomes the main peak. Diffraction profile in Figure 7 exhibits much less preferred orientation, which has a sharp contrast with the data of thin film. The GIXD patterns in Figure 7 are similar to that reported for bulk PEN.<sup>23</sup> This fact indicates that the preferential crystal orientation hardly occurs in very thick or bulk PEN film.

In situ measurements during heating of the PEN thin films were also conducted by employing the synchrotron facility at SPring-8. Because of the relatively longer measuring time for each scan compared with that of IR, we only carried out the temperature-dependent GIXD measurements under out-of-plane scan mode. For the experimental condition with  $\lambda = 0.7\text{ \AA}$ , the critical angle for PEN is about  $0.08^\circ$ . So we chose the incident angle of  $0.1^\circ$  for the bulk-sensitive measurements. Figure 8 shows the development of the GIXD profiles of a  $75\text{ nm}$  PEN film at different temperatures. Even though the slight damage from the synchrotron radiation became detectable as the proceeding of experiments (from the decrease in the overall intensity of the two Bragg peaks (100) and (110)), analyzing the change of the relative intensities for (100) and (110) peaks can still provide us useful information about the structural development during crystallization. At  $130\text{ }^\circ\text{C}$ , the absence of Bragg peak suggests an amorphous state. With elevating temperature to 170 and then  $200\text{ }^\circ\text{C}$  and subsequently cooling back to room temperature, Bragg peaks (100) and (110) can be observed and their relative intensities decrease. As already mentioned, the (110) lattice plane is approximately parallel to the naphthalene ring in PEN molecule, and the (100) plane aligns parallel to  $b$  and  $c$  axes. Taking into account the in situ data of RAIR, the present GIXD results acquired in the out-of-plane mode may reflect the difference in coplanarity with respect to the film surface: during the heating and subsequent cooling process, the naphthalene ring rotates to be more parallel to the

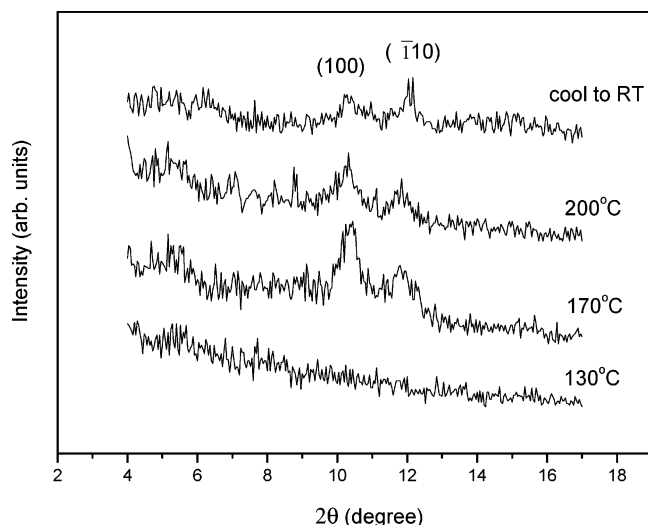


**Figure 8.** Temperature dependence of the out-of-plane GIXD profiles of a 75 nm PEN thin film during heating and subsequent cooling to room temperature. (incident angle  $\alpha = 0.1^\circ$ ).

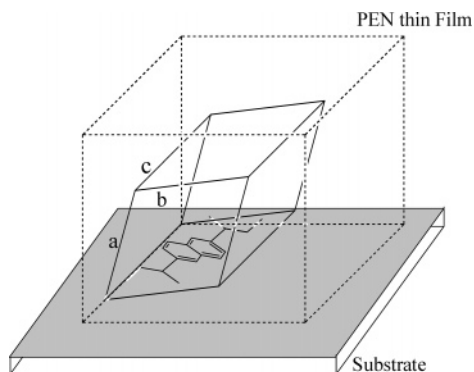


**Figure 9.** Schematic representation for the  $\alpha$ -form crystal structure of PEN in thin film, on the basis of structural analysis by Mencik<sup>23</sup> and our RAIR and GIXD results.

surface than the (100) plane due to the existence of an angle between (110) and (100) planes. The schematic representation for  $\alpha$ -form crystal structure of PEN in a thin film is plotted as Figure 9, in which the possible arrangement in the molecular chain of PEN on substrate is also illuminated.

The anisotropic distribution of molecular structure in polymer as found in our study have also been reported for other polymeric systems and surface-induced effect was supposed to contribute greatly to the observations.<sup>36–42</sup> Because near interfacial boundaries, surface, and interface effects may lead to physical properties that significantly differ from those in the bulk. Factor et al.<sup>14</sup> studied the near surface structure of an aromatic polyimide film and found that within the first 90 Å from the surface the ordering of the polymer molecules is markedly enhanced. The surface ordering of aliphatic chains was also observed in a molecular simulation study. Ito et al.<sup>43</sup> studied the crystallization of a free-standing thin film by means of the molecular dynamics simulation of a united atom model of PE in continuous space. Following the rapid quenching of a free-standing thin film from 500 to 300 K, crystals nucleated spontaneously, and independently, at both surfaces, with the long axis of the crystalline chains oriented in the plane of the thin film. The independently nucleated crystals grew by propagation into the interior of the thin film from both surfaces. For the present study, we can also take the surface-induced effect as a possible reason for the experimental results if considering the fact that role of the surface or interface is usually more

important in thin film than in bulk as a whole. Another possible reason is the confinement effect. When the confining dimensions start to approach the length scale of the lamellar thickness of the polymer crystals, anomalous behaviors such as slowing down of the crystal growth or orientation may be expected. It should be noted that the buried polymer–substrate interface can also play a part for the anisotropic crystal orientation in PEN ultrathin films. However, taking into account the coincidence of the crystal orientation obtained from both GIXD and RAIR profiles despite of the different substrates of PEN film used in the two methods (silicon wafer for GIXD and gold-coated glass wafer for RAIR), the effect of the polymer–substrate interface on the orientation might be relatively weak.

#### 4. Conclusions

The molecular orientation of PEN thin films has been investigated by the combination of RAIR and GIXD techniques during isothermal and nonisothermal crystallization. It is concluded that the naphthalene ring and C=O of PEN molecule in thin films are prone to aligning parallel to the film surface during the formation of  $\alpha$ -form crystals, while it is not the case for the thicker films. The results also suggested that in situ RAIR can be a convenient tool to investigate the detailed development of the orientation and crystallization processes by adopting orientation-sensitive and crystallization- (or conformation-) sensitive bands respectively. The developing speeds of the orientation for the naphthalene and C=O appear clearly faster than the crystallization rate. In situ GIXD measurements using synchrotron radiation revealed that the naphthalene ring rotates to be more parallel to the surface than the lattice plane containing *b* and *c* axes ((100) plane) during the nonisothermal crystallization. Surface-induced effect and confinement effect were proposed to be the possible reasons for the observed orientation in PEN thin films.

**Acknowledgment.** We would like to thank Prof. Deyan Shen of Institute of Chemistry, Chinese Academy of Sciences, for providing the PEN samples. We also thank Prof. H. Terauchi of Kwansei Gakuin University for fruitful discussion. The synchrotron radiation experiments were performed at the BL13XU in SPring-8 with the approval of the Japan Synchrotron Radiation Research Institute (JASRI) (Proposal No. 2006B1201).

#### References and Notes

- (1) Keddie, J. L.; Jones, R. A. L.; Cory, R. A. *Faraday Discuss.* **1994**, *98*, 219.
- (2) Forrest, J. A.; Dalnoki-Veress, K.; Stevens, J. R.; Dutcher, J. R. *Phys. Rev. Lett.* **1996**, *77*, 2002.
- (3) Tsui, O. K. C.; Russell, T. P.; Hawker, C. J. *Macromolecules* **2001**, *34*, 5535.
- (4) Frank, C. W.; Rao, V.; Despotopoulou, M. M.; Pease, R. F. W.; Hinsberg, W. D.; Miller, R. D.; Rabolt, J. F. *Science* **1996**, *273*, 912.
- (5) Schonherr, H.; Frank, C. W. *Macromolecules* **2003**, *36*, 1188.
- (6) Krausch, G.; Dai, C.-A.; Kramer, E. J.; Marko, J. F.; Bates, F. S. *Macromolecules* **1993**, *26*, 5566.
- (7) Tao, H.-J.; Meuse, C. W.; Yang, X.; MacKnight, W. J.; Hsu, S. L. *Macromolecules* **1994**, *27*, 7146.
- (8) Ludwigs, S.; Schmidt, K.; Stafford, C. M.; Amis, E. J.; Fasolka, M. J.; Karim, A.; Magerle, R.; Krausch, G. *Macromolecules* **2005**, *38*, 1850.
- (9) Liang, T.; Makita, Y.; Kimura, S. *Polymer* **2001**, *42*, 4867.
- (10) Prest, W. M.; Luca, Jr. D. J. *J. Appl. Phys.* **1980**, *51*, 5170.
- (11) Despotopoulou, M. M.; Miller, R. D.; Rabolt, J. F.; Frank, C. W. *J. Polym. Sci., Part B: Polym. Phys.* **1996**, *34*, 2335.
- (12) Cohen, Y.; Reich, S. *J. Polym. Sci.: Polym. Phys. Ed.* **1981**, *19*, 599.
- (13) Francis, S. A.; Ellison, A. H.; Ellison, J. *Opt. Soc. Am.* **1959**, *49*, 131.
- (14) Factor, B. J.; Russell, T. P.; Toney, M. F. *Phys. Rev. Lett.* **1991**, *66*, 1181.
- (15) Factor, B. J.; Russell, T. P.; Toney, M. F. *Macromolecules* **1993**, *26*, 2847.

- (16) Yakabe, H.; Tanaka, K.; Nagamura, T.; Sasaki, S.; Sakata, O.; Takahara, A.; Kajiyama, T. *Polym. Bull. (Berlin)* **2005**, *53*, 213.
- (17) Toney, M. F.; Russell, T. P.; Logan, J. A.; Kikuchi, H.; Sands, J. M.; Kumar, S. K. *Nature* **1995**, *374*, 709.
- (18) Durell, M.; Macdonald, J. E.; Trolley, D.; Wehrum, A.; Jukes, P. C.; Jones, R. A. L.; Walker, C. J.; Brown, S. *Europhys. Lett.* **2002**, *58*, 844.
- (19) Zhang, Y.; Zhang, J.; Lu, Y.; Duan, Y.; Yan, S.; Shen, D. *Macromolecules* **2004**, *37*, 2532.
- (20) Parratt, L. G. *Phys. Rev.* **1954**, *95*, 359.
- (21) Kressler, J.; Wang, C.; Kammer, H. W. *Langmuir* **1997**, *13*, 4407.
- (22) Harrick, N. J. *Internal Reflection Spectroscopy*, 2nd ed.; Harrick Scientific Corp.: New York **1979**.
- (23) Mencik, Z. *Chem. Prum.* **1976**, *17*, 78.
- (24) Buchner, S.; Wiswe, D.; Zachmann, H. G. *Polymer* **1989**, *30*, 480.
- (25) Ouchi, I.; Hosoi, M.; Shimotsuna, S. *J. Appl. Polym. Sci.* **1977**, *21*, 3445.
- (26) Zhang, Y.; Mukoyama, S.; Mori, K.; Shen, D.; Yan, S.; Ozaki, Y.; Takahashi, I. *Surf. Sci.* **2006**, *600*, 1559.
- (27) Iwamoto, R.; Ohta, K. *Appl. Spectrosc.* **1984**, *38*, 359.
- (28) Wang, S.; Shen, D.; Qian, R. *J. Appl. Polym. Sci.* **1996**, *60*, 1385.
- (29) Bullions, T. A.; Wei, M.; Porbeni, F. E.; Gerber, M. J.; Peet, J.; Balik, M.; White, J. L.; Tonelli, A. E. *J. Polym. Sci.: Polym. Phys. Ed.* **2002**, *40*, 992.
- (30) Zhang, Y.; Lu, Y.; Duan, Y.; Zhang, J.; Yan, S.; Shen, D. *J. Polym. Sci.: Polym. Phys. Ed.* **2004**, *42*, 4440.
- (31) Yan, C.; Li, H.; Zhang, J.; Ozaki, Y.; Shen, D.; Yan, D.; Shi, A.; Yan, S. *Macromolecules* **2006**, *39*, 8041.
- (32) Strobl, Gert. R. *The physics of polymers: concepts for understanding their structures and behavior*, 2nd ed.; Springer, Berlin, New York, 1997.
- (33) Kimura, F.; Kimura, T.; Sugisaki, A.; Komatsu, M.; Sata, H.; Ito, E. *J. Polym. Sci.: Polym. Phys. Ed.* **1997**, *35*, 2741.
- (34) Vasanathan, N.; Salem, D. R. *Macromolecules* **1999**, *32*, 6319.
- (35) Cakmak, M.; Lee, S. W. *Polymer* **1995**, *36*, 4039.
- (36) Jukes, P. C.; Das, A.; Durell, M.; Trolley, D.; Higgins, A. M.; Geoghegan, M.; Macdonald, J. E.; Jones, R. A. L.; Brown, S.; Thompson, P. *Macromolecules* **2005**, *38*, 2315.
- (37) Saraf, R. F.; Dimitrakopoulos, C.; Toney, M. F.; Kowalczyk, S. P. *Langmuir* **1996**, *12*, 2802.
- (38) Kawamoto, N.; Mori, H.; Nitta, K.; Sasaki, S.; Yui, N.; Terano, M. *Angew. Makromol. Chem.* **1998**, *256*, 69.
- (39) Kawamoto, N.; Mori, H.; Nitta, K.; Sasaki, S.; Yui, N.; Terano, M. *Macromol. Chem. Phys.* **1998**, *199*, 261.
- (40) Nishino, T.; Matsumoto, T.; Nakamae, K. *Polym. Eng. Sci.* **2000**, *40*, 336.
- (41) Capitan, M. J.; Rueda, D. R.; Ezquerro, T. A. *Macromolecules* **2004**, *37*, 5653.
- (42) Liang, Y.; Lee, H. S. *Macromolecules* **2005**, *38*, 9885.
- (43) Ito, M.; Matsumoto, M.; Doi, M. *Fluid Phase Equilib.* **1998**, *144*, 395.

MA070021E